Enhanced future variability during India's rainy season

Arathy Menon,[1,2] Anders Levermann,[1,2] and Jacob Schewe[1]

[1]   The Indian summer monsoon shapes the livelihood of a large share of the world's population. About 80% of annual precipitation over India occurs during the monsoon season from June through September. Next to its seasonal mean rainfall, the day-to-day variability is crucial for the risk of flooding, national water supply, and agricultural productivity. Here we show that the latest ensemble of climate model simulations, prepared for the AR-5 of the Intergovernmental Panel on Climate Change, consistently projects significant increases in day-to-day rainfall variability under unmitigated climate change. The relative increase by the period 2071–2100 with respect to the control period 1871–1900 ranges from 13% to 50% under the strongest scenario (Representative Concentration Pathways, RCP-8.5), in the 10 models with the most realistic monsoon climatology; and 13% to 85% when all the 20 models are considered. The spread across models reduces when variability increase per degree of global warming is considered, which is independent of the scenario in most models, and is 8% ± 4%/K on average. This consistent projection across 20 comprehensive climate models provides confidence in the results and suggests the necessity of profound adaptation measures in the case of unmitigated climate change. **Citation:** Menon, A., A. Levermann, and J. Schewe (2013), Enhanced future variability during India's rainy season, *Geophys. Res. Lett.*, *40*, 3242–3247, doi:10.1002/grl.50583.

1.   Introduction

[2]   Indian summer monsoon rainfall exhibits significant variability within the rainy season, which has great impact on agricultural productivity as well as the national economy of India as a whole [*Parthasarathy et al.*, 1988; *Auffhammer et al.*, 2006; *Guhathakurta et al.*, 2011]. Changes in both seasonal mean precipitation [*Guhathakurta and Rajeevan*, 2008] and the number of extreme rainfall events [*Goswami et al.*, 2006; *Rajeevan et al.*, 2008] have been observed, but a clear attribution to physical causes is difficult. A 131 year observational record covering the whole of India shows no clear evidence that either the seasonal mean or the interannual variability of all Indian summer monsoon rainfall is affected by global warming [*Kripalani et al.*, 2003]. However, a daily gridded rainfall data set over a smaller region over Central India exhibits an increasing trend in the extreme rainfall events for the past few decades, even though the seasonal mean rainfall does not show a significant trend [*Goswami et al.*, 2006].

[3]   A subset of the coupled general circulation models that participated in the Coupled Model Intercomparison Project phase 3 (CMIP-3) show an increase in the south Asian monsoon rainfall [*Turner and Annamalai*, 2012] as well as a weakening of the large scale monsoon circulation during the 21st and 22nd centuries in response to a transient increase in anthropogenic radiative forcing [*Ueda et al.*, 2006; *Fan et al.*, 2012]. The percentage change in global mean precipitation per degree change in temperature is simulated consistently by most of the climate models [*Held and Soden*, 2006; *Lambert and Webb*, 2008], but on a regional scale in India, these models in general do not agree on the changes in precipitation in response to changes in global mean surface temperature [*Lal et al.*, 1998]: Some of them project a positive trend in the South Asian monsoon rainfall and its variability under global warming [*Meehl and Washington*, 1993; *Kitoh et al.*, 1997; *Hu et al.*, 2000; *Lal et al.*, 2001], which is mainly attributed to the enhanced moisture flux into the Indian region due to an increase in the atmospheric moisture content and the enhanced evaporation over the Arabian Sea and the equatorial Indian Ocean in response to global warming [*May*, 2011], whereas a study based on a high resolution nested model suggests a suppression of monsoon precipitation in the 21st century in response to the weakening of the large scale monsoon circulation as well as a suppression of the intraseasonal modes [*Ashfaq et al.*, 2009]. Even though low-frequency large-scale processes like El Niño-Southern Oscillation (ENSO) can contribute to the large-scale projection of Indian summer monsoon rainfall, seasonal precipitation also depends on subseasonal variability, which are largely determined by internal dynamics [*Turner and Annamalai*, 2012].

[4]   Subseasonal variability comprises a wide range of atmospheric phenomena, e.g., active and break spells [*Rajeevan et al.*, 2006], lows and depressions [*Goswami*, 2005], and Madden-Julian oscillation [*Lin et al.*, 2008]. Individual model projections using HadCM3 and ECHAM4/OPYC3 coupled model suggest a decrease in the number of wet days, whereas the mean intensity of daily precipitation during the monsoon season increases [*Semenov and Bengtsson*, 2002; *Turner and Slingo*, 2009]. Time-slice experiments using ECHAM4 atmospheric general circulation model show a general increase in the frequency of heavy rainfall events [*May*, 2004] over the tropical Indian Ocean, northwest India, and northeast India. Active and break events show a projected intensification relative to the seasonal cycle [*Turner and Slingo*, 2009; *Turner and Annamalai*, 2012] in some coupled modeling studies. But a study based on a subset of the CMIP-3 models shows that the response of the duration of active/break spells to climate
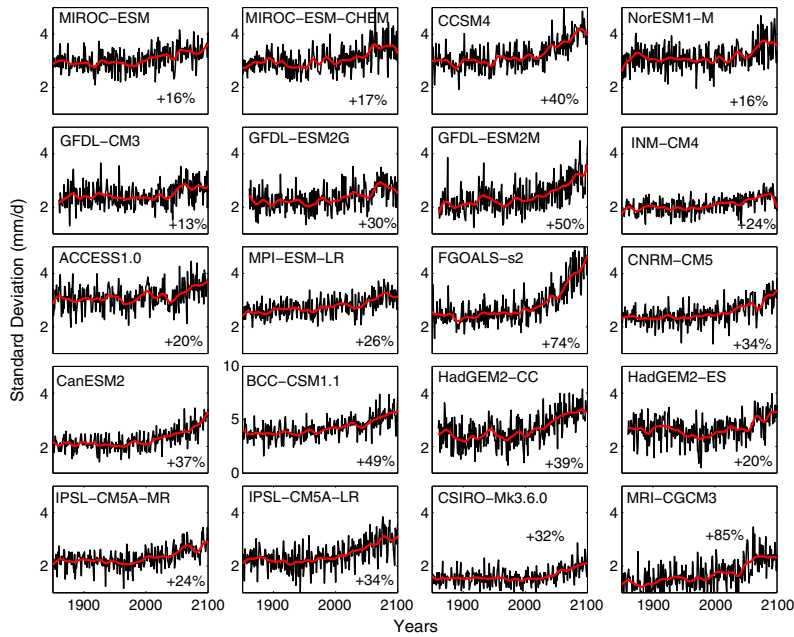

Figure 1. Time series of subseasonal standard deviation of all India summer (June–September) monsoon rainfall for the 20 comprehensive climate models for RCP-8.5 scenario. The variability (σ) is computed as the root-mean-square of the daily deviation from the seasonal mean of each individual year. Please note that the y-axis range is different (0–10 mm/d) for BCC-CSM1.1. The nonlinear trend in seasonal standard deviation from a singular spectrum analysis method [*Moore et al.*, 2005] is shown (red line) and the percentages show the relative change in standard deviation in the future with respect to the past, i.e., $(\bar{\sigma}_{2071—2100} - \bar{\sigma}_{1871—1900})/\bar{\sigma}_{1871—1900}$.

change is even inconsistent among the same models for different scenarios [*Mandke et al.*, 2007]. In this study we examine changes in the subseasonal variability associated with day-to-day variability of Indian summer monsoon rainfall under global warming scenarios.

2. Data and Methods

[5] Here we analyze global warming simulations carried out with 20 models participating in the Coupled Model Intercomparison Project phase 5 (CMIP-5) [*Taylor et al.*, 2012]. Historical simulations are based on observed concentrations of green house gases and reconstructed aerosol emissions. Future projections are based on the four Representative Concentration Pathways (RCP) [*Moss et al.*, 2010]. RCP-4.5 is the pathway for which radiative forcing reaches $4.5\,\mathrm{W\,m^{-2}}$ by 2100. Similarly RCP-8.5 and RCP-6.0 represent the pathways for which radiative forcing reach 8.5 and $6\,\mathrm{W\,m^{-2}}$ in 2100. RCP-2.6 peaks in radiative forcing at $3\,\mathrm{W\,m^{-2}}$ before 2100 and declines afterward reaching $2.6\,\mathrm{W\,m^{-2}}$ in 2100. The models are selected such that the daily rainfall data is available for the historic period (1850–2005), RCP-8.5 scenario, and at least one more scenario at the time of the study. In this analysis we use the term subseasonal variability to refer in general to the standard deviation of the daily rainfall, which can include contributions from various factors like individual heavy rainstorms, lows and depressions [*Goswami*, 2005], active/break cycles [*Rajeevan et al.*, 2006], and intraseasonal oscillations [*Goswami and Ajaya Mohan*, 2001]. Subseasonal variability of the June–September (JJAS) rainfall is calculated as the root-mean-square of the daily deviation for each individual
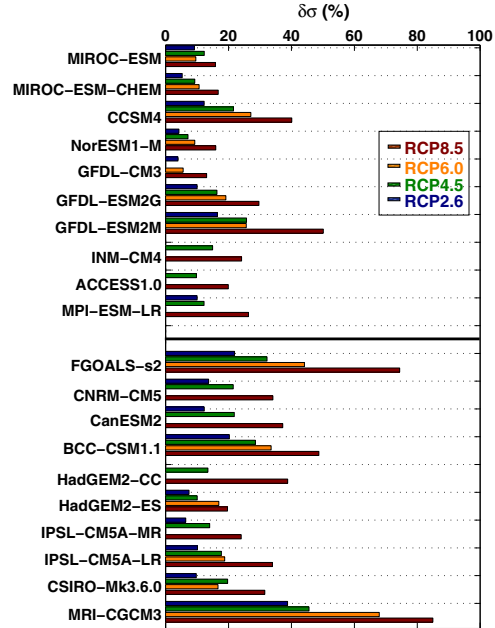
Figure 2. Percentage change of standard deviation as per Figure 1 by the end of the 21st century compared to the past for different models under the four RCPs. Change in subseasonal standard deviation is positive for all the models for all the scenarios. The gap and the black horizontal line between the bars for MPI-ESM-LR and FGOALS-s2 separate the models into two groups, i.e., those above (below) the gap having seasonal mean rainfall within (outside) twice the standard deviation of the observed mean (refer to Figure 3 for more details).
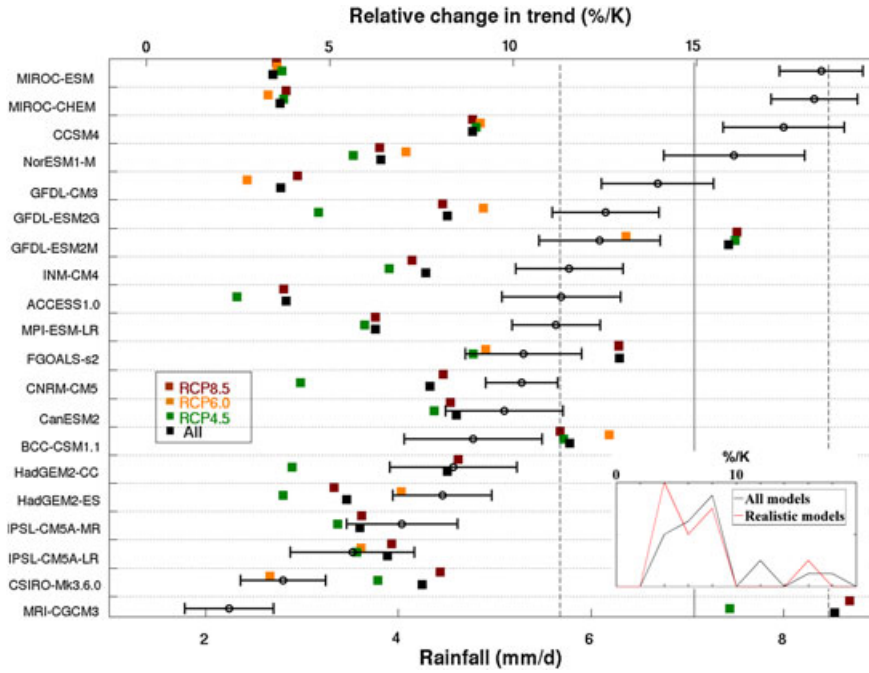
Figure 3. Slopes of the linear trend lines (colored squares, upper *x*-axis) from the scatter plots (Figure 4) between δT and σ. The black vertical line shows the all-India mean monsoon rainfall from observations for the period 1871–2004, and the dashed lines show mean plus/minus twice the standard deviation of all-India mean rain. Black circles with error bars represent mean and mean plus/minus one standard deviation for the 20 comprehensive models from 1871 to 2004 (lower *x*-axis). The inset figure shows the normalized histograms for the black squares (slopes of all scenarios combined) for all 20 models (black line) and the 10 most realistic models (red line).

year from the seasonal mean rainfall averaged over the India land region. Relative changes in the subseasonal variability is computed as the difference in mean subseasonal variability between the end of the 21st century (2071–2100) and the end of the 19th century (1871–1900) divided by the subseasonal variability during the end of the 19th century.

3. Results

[6] Subseasonal variability of daily rainfall averaged over the whole of India shows a significant increase from the mid-19th century to the end of the 21st century under the RCP-8.5 scenario (Figure 1). The percentages in each panel represent the relative changes ($\delta\sigma$) of the standard deviation σ of daily rainfall within the monsoon season (June–September) from the end of the 19th century (1871–1900) to the end of the 21st century (2071–2100). $\delta\sigma$ for the high concentration scenario, RCP-8.5, shows an increase of 13 to 50% compared to the historic period for the most realistic models (Figure 3) and 13 to 85% for the 20 models under consideration (for details of the models used in the study, please refer to the supporting information, Table S1). Similarly an increase in subseasonal variability is also found under all four Representative Concentration Pathways (RCPs), which were designed to span the full range of future warming scenarios [*Moss et al.*, 2010] (see Figure 2). $\delta\sigma$ is highest under RCP-8.5 and lowest under RCP-2.6 for all those models which have data available for these two scenarios. Hence, generally across models and concentration pathways, we find a robust tendency that sub-

seasonal variability shows an increase with global mean temperature (Figure 4).

[7] While all models show an increase in day-to-day variability, some models are more realistic in capturing the observed seasonal mean rainfall over India than others (Figure 3). The all India June–September (JJAS) climatological mean rainfall from observations [*Parthasarathy*

Table 1. Dependence of σ on δT[a]

Model	Trend (%/K)			
	RCP-8.5	RCP-6.0	RCP-4.5	All Scenarios
MIROC-ESM	4	4	4	3
MIROC-ESM-CHEM	4	3	4	4
CCSM4	9	9	9	9
NorESM1-M	6	7	6	6
GFDL-CM3	4	3		4
GFDL-ESM2G	8	9	5	8
GFDL-ESM2M	16	13	16	16
INM-CM4	7		7	8
ACCESS1.0	4		2	4
MPI-ESM-LR	6		6	6
FGOALS-s2	13	9	9	13
CNRM-CM5	8		4	8
CanESM2	8		8	8
BCC-CSM1.1	11	13	11	12
HadGEM2-CC	8		4	8
HadGEM2-ES	5	7	4	5
IPSL-CM5A-MR	6		5	6
IPSL-CM5A-LR	7	6	6	7
CSIRO-Mk3.6.0	8	3	6	8
MRI-CGCM3	19		16	19

[a]Slopes of the regression are listed from scatter plots for each RCP separately and for combined scenarios (compare Figure 4).
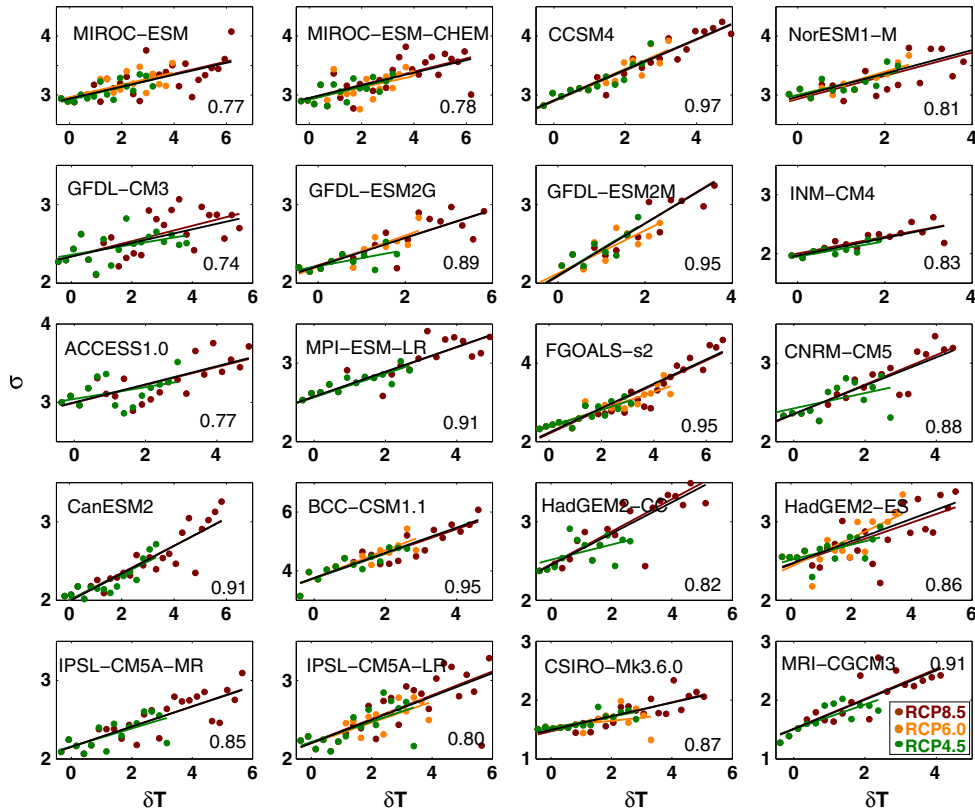
Figure 4. Scatter plot between σ and δT for RCP-8.5(red dots), RCP-6.0(orange dots), and RCP-4.5(green dots) for the 20 comprehensive climate models. Here each value represents the average value of σ over a δT interval of 0.25°C. Red, orange, green, and black lines represent the linear trend for RCP-8.5, RCP-6.0, RCP-4.5, and a combination of all the three scenarios together, respectively. The numbers on each panel represent the r-values for the combination of all the three scenarios (black line).

et al., 1994] for the period 1871 to 2004 is 7.1 mm/day (vertical black line in Figure 3) with a standard deviation of 0.7 mm/day or about 10% of the period's mean. While no model's monsoon rainfall exceeds the observed value by more than two standard deviations, half of the models simulate a significantly weaker monsoon than observed. Spectral analysis of model data and daily observational rainfall data [*Rajeevan et al.*, 2006] for the period 1951 to 2005 shows that majority of the models tend to produce the time scales of subseasonal variability realistically (Please refer to supporting information, Figures S1 and S2). Observational data as well as majority of the models capture significant powers at synoptic scale period (< 10 days) and quasi-biweekly period (10–20 days). The low frequency intraseasonal oscillations (ISO), like the nortward-propagating 30–60 day modes, are not significant in the observational data set at 95% confidence level of the red noise spectrum (Figure S1). Area-averaging of rainfall over the all-India region, a much larger domain compared to the ISO spatial scale, might be the reason behind the insignificant spectral peaks at low-frequency intraseasonal time scales. It is also noted that the models with more realistic seasonal mean rainfall capture the annual cycle well comparable with the observations (Figure S3). Table 1 lists the linear trends in the subseasonal variability per global temperature increase δT for each scenario and all scenarios combined. The trends for RCP-2.6 are not shown as δT is below 2°C for this concentration pathway for most of the models, and hence,

no robust trend can be estimated. All models consistently show an increase in σ with increase in temperature but with differing slopes (Figure 4) under all the RCP scenarios. In most of the models, the increase in subseasonal variability per degree is very similar for all RCPs, indicating a robust relationship with global mean temperature irrespective of the scenario. On average the models yield an increase in variability in the range 8% ± 4% (*median ± inter*-model standard deviation from the last column of Table 1) per degree of global warming. The correlation coefficient between σ and δT is large for most of the models. The regression of the increase in variability binned over temperature increase shows r-values between 74% and 97% for the combination of all RCP scenarios (Figure 4) for the models under consideration.

4. Conclusions

[8] In summary, we find an increase in subseasonal variability of the Indian summer monsoon rainfall with increasing global mean temperature consistently across the CMIP-5 climate model ensemble under different concentration pathways. To first order, this increase can be considered independent of the pathway through which the temperature change is reached, but varies between models, with a most likely range of 8% ± 4% per degree of warming.

[9] The increase in day-to-day variability can be associated with an increase in the extreme rainfall events.

Agriculture depends strongly on the periodicity and distribution of rainfall within the growing season. Extreme events associated with day-to-day variability of monsoon rainfall can cause floods and thereby lead to serious socioeconomic problems. Hence, the projected change of the day-to-day variability of rainfall is of critical importance. The CMIP-3 models show a wide range of skill in simulating the intraseasonal oscillations [*Lin et al.*, 2008; *Sperber and Annamalai*, 2008], but they generally project an increase in the number of extreme precipitation events under anthropogenic warming [*Allan and Soden*, 2008]. Our results are consistent with projected increases in extreme rainfall events that have been partly attributed to the increase in water holding capacity of the atmosphere and higher precipitable water content associated with warming [*Fowler and Hennessy*, 1995; *Turner and Slingo*, 2009] as well as the upper-tropospheric cooling that destabilizes the atmosphere and enhances precipitation [*Lau et al.*, 2005]. The dynamical effect also plays a role in enhancing the extreme events [*Chen et al.*, 2012]. The surface fluxes from ocean increases due to a warmer sea surface temperature, which can lead to an increase in the moisture supply resulting in the "rich-get-richer" mechanism that will enhance the precipitation over regions that already have strong moisture convergence and enhances convection which can increase the precipitation intensity. The robustness of the trend across climate models provides confidence that an increase in day-to-day rainfall variability within India's rainy season is to be expected under unabated climate change. The subseasonal variability presented here can have strong regional variability. The coarse spatial resolution of the global models applied here (∼2 degrees for many models) does not necessarily allow for a robust representation of the spatial pattern, which is thus beyond the scope of this study. Spatial variability should be kept in mind while designing adaptation methods as the adaptation criteria depend on vulnerability, demography, land use pattern, etc. Regional models of higher spatial resolution might be better suited to study the spatial variability of subseasonal monsoon rainfall.

References

Allan, R., and B. Soden (2008), Atmospheric warming and the amplification of precipitation extremes, *Science*, *321*(5895), 1481–1484.

Ashfaq, M., Y. Shi, W. Tung, R. J. Trapp, X. Gao, J. S. Pal, and N. S. Diffenbaugh (2009), Suppression of South Asian summer monsoon precipitation in the 21st century, *Geophys. Res. Lett.*, *36*, L01704, doi:10.1029/2008GL036500.

Auffhammer, M., V. Ramanathan, and J. R. Vincent (2006), Integrated model shows that atmospheric brown clouds and greenhouse gases have reduced rice harvests in India, *Proc. Natl. Acad. Sci. U. S. A.*, *103*, 19,668–19,672.

Chen, C. A., C. Chou, and C. T. Chen (2012), Regional perspective on mechanisms for tropical precipitation frequency and intensity under global warming, *J. Clim.*, *25*, 8487–8501.

Fan, F., M. Mann, S. Lee, and J. Evans (2012), Future changes in the South Asian summer monsoon: An analysis of the CMIP3 multi-model projections, *J. Clim.*, *25*(11), 3909–3928.

Fowler, A. M., and K. J. Hennessy (1995), Potential impacts of global warming on the frequency and magnitude of heavy precipitation, *Nat. Hazards*, *11*(3), 283–303.

Goswami, B. N. (2005), South Asian monsoon, in *Intraseasonal Variability in the Atmosphere-Ocean Climate System*, edited by Lau, W. K. M., and D. E. Waliser, Springer, Berlin, pp. 19–61.

Goswami, B. N., and R. S. Ajaya Mohan (2001), Intraseasonal oscillations and interannual variability of the Indian summer monsoon, *J. Clim.*, *14*(6), 1180–1198.

Goswami, B. N., V. Venugopal, D. Sengupta, M. S. Madhusoodanan, and P. K. Xavier (2006), Increasing trend of extreme rain events over India in a warming environment, *Science*, *314*, 1442–1445.

Guhathakurta, P., and M. Rajeevan (2008), Trends in the rainfall pattern over India, *Int. J. Climatol.*, *28*(11), 1453–1469.

Guhathakurta, P., O. P. Sreejith, and P. A. Menon (2011), Impact of climate change on extreme rainfall events and flood risk in India, *J. Earth Syst. Sci.*, *120*(3), 359–373.

Held, I., and B. Soden (2006), Robust responses of the hydrological cycle to global warming, *J. Clim.*, *19*(21), 5686–5699.

Hu, Z., M. Latif, E. Roeckner, and L. Bengtsson (2000), Intensified Asian summer monsoon and its variability in a coupled model forced by increasing greenhouse gas, *Geophys. Res. Lett.*, *27*(17), 2681–2684.

Kitoh, A., S. Yukimoto, A. Noda, and T. Motoi (1997), Simulated changes in the Asian summer monsoon at times of increased atmospheric CO_2, *J. Meteorol. Soc. Jpn.*, *75*(6), 1019–1031.

Kripalani, R. H., A. Kulkarni, S. S. Sabade, and M. L. Khandekar (2003), Indian monsoon variability in a global warming scenario, *Nat. Hazards*, *29*(2), 189–206.

Lal, M., P. H. Whetton, A. B. Pittock, and B. Chakraborty (1998), Simulation of present-day climate over the Indian subcontinent by general circulation models, *Terr. Atmos. Oceanic Sci.*, *9*, 69–96.

Lal, M., T. Nozawa, S. Emori, H. Harasawa, K. Takahashi, M. Kimoto, A. Abe-Ouchi, T. Nakajima, T. Takemura, and A. Numaguti (2001), Future climate change: Implications for Indian summer monsoon and its variability, *Curr. Sci.*, *81*(9), 1196–1207.

Lambert, F. H., and M. J. Webb (2008), Dependency of global mean precipitation on surface temperature, *Geophys. Res. Lett.*, *35*, L16706, doi:10.1029/2008GL034838.

Lau, K. M., H. T. Wu, Y. C. Sud, and G. K. Walker (2005), Effects of cloud microphysics on tropical atmospheric hydrologic processes and intraseasonal variability, *J. Clim.*, *18*(22), 4731–4751.

Lin, J. L., K. M. Weickman, G. N. Kiladis, B. E. Mapes, S. D. Schubert, M. J. Suarez, J. T. Bacmeister, and M. I. Lee (2008), Subseasonal variability associated with Asian summer monsoon simulated by 14 IPCC AR4 coupled GCMs, *J. Clim.*, *21*(18), 4541–4567.

Mandke, S. K., A. K. Sahai, M. A. Shinde, S. Joseph, and R. Chattopadhyay (2007), Simulated changes in active/break spells during the Indian summer monsoon due to enhanced CO_2 concentrations: Assessment from selected coupled atmosphere-ocean global climate models, *Int. J. Climatol.*, *27*(7), 837–859.

May, W. (2004), Simulation of the variability and extremes of daily rainfall during the Indian summer monsoon for present and future times in a global time-slice experiment, *Clim. Dyn.*, *22*(2), 183–204.

May, W. (2011), The sensitivity of the Indian summer monsoon to a global warming of 2°C with respect to pre-industrial times, *Clim. Dyn.*, *37*(9), 1843–1868.

Meehl, G. A., and W. M. Washington (1993), South Asian summer monsoon variability in a model with doubled atmospheric carbon dioxide concentration, *Science*, *260*, 1101–1104.

Moore, J. C., A. Grinsted, and S. Jevrejeva (2005), New tools for analyzing time series relationships and trends, *Eos Trans. AGU*, *86*(24), 226–232.

Moss, R. H., et al. (2010), The next generation of scenarios for climate change research and assessment, *Nature*, *463*, 747–756.

Parthasarathy, B., A. Munot, and D. Kothawale (1988), Regression model for estimation of Indian foodgrain production from summer monsoon rainfall, *Agric. For. Meteorol.*, *42*(2-3), 167–182, doi:10.1016/0168-1923(88)90075-5.

Parthasarathy, B., A. Munot, and D. Kothawale (1994), All-India monthly and seasonal rainfall series: 1871–1993, *Theor. Appl. Climatol.*, *49*(4), 217–224.

Rajeevan, M., J. Bhate, and A. Jaswal (2008), Analysis of variability and trends of extreme rainfall events over India using 104 years of gridded daily rainfall data, *Geophys. Res. Lett.*, *35*, L18707, doi:10.1029/2008GL035143.

Rajeevan, M., J. Bhate, J. A. Kale, and B. Lal (2006), High resolution daily gridded rainfall data for the Indian region: Analysis of break and active monsoon spells, *Curr. Sci.*, *91*(3), 296–306.

Semenov, V., and L. Bengtsson (2002), Secular trends in daily precipitation characteristics: Greenhouse gas simulation with a coupled AOGCM, *Clim. Dyn.*, *19*(2), 123–140.

Sperber, K., and H. Annamalai (2008), Coupled model simulations of boreal summer intraseasonal (30–50 day) variability, Part 1: Systematic errors and caution on use of metrics, *Clim. Dyn.*, *31*(2), 345–372.

Taylor, K., R. Stouffer, and G. Meehl (2012), An overview of CMIP5 and the experiment design, *Bull. Am. Meteorol. Soc.*, *93*(4), 485–498.

Turner, A., and H. Annamalai (2012), Climate change and the South Asian summer monsoon, *Nat. Clim. Change*, *2*, 587–595.

Turner, A., and J. Slingo (2009), Subseasonal extremes of precipitation and active-break cycles of the Indian summer monsoon in a climate-change scenario, *Q. J. R. Meteorol. Soc.*, *135*(640), 549–567.

Ueda, H., A. Iwai, K. Kuwako, and M. Hori (2006), Impact of anthropogenic forcing on the Asian summer monsoon as simulated by eight GCMs, *Geophys. Res. Lett.*, *33*, L06703, doi:10.1029/2005GL025336.